Impact of ion concentration on Alamine 336 degradation in uranium solvent extraction processes

W.S. Gaeseb[1], V.L. Ndeshimona[1]*, O. T. Johnson[1,2]

1 University of Namibia, Faculty of Agriculture, Engineering and Natural Sciences, School of Engineering and the Built Environment, Department of Mechanical and Metallurgical Engineering, P.O. Box 3624, Ongwediva, Namibia

2 University of South Africa, School of Engineering and Built Environment, Department of Chemical and Materials Engineering, Pretoria, South Africa.

*vamuthenu@unam.na

Abstract

The degradation of Alamine 336, a critical extractant in uranium solvent extraction (SX) processes, is a significant challenge at the Rossing Uranium Limited (RUL) processing plant. This study investigates the impact of ion concentrations—specifically chloride, nitrate, ferrous, and manganese ions—on the degradation of Alamine 336 in the SX circuit. Through a 2^{k-p} fractional factorial design, the study evaluates the interactions of these ions, aiming to identify key contributors to solvent degradation. The findings reveal that nitrate and chloride ions are significant predictors of Alamine 336 degradation, with higher concentrations leading to increased solvent breakdown. Manganese and ferrous ions also play a role, with manganese exhibiting an oxidizing effect that exacerbates degradation. The study further identifies nitrosamine formation as a primary degradation product, supporting previous research. By employing regression analysis, the study develops a model to predict Alamine concentration based on ion concentrations, offering a valuable tool for optimizing uranium extraction efficiency and mitigating solvent degradation. These results underscore the importance of maintaining controlled ion concentrations, particularly keeping redox potential below 500 mV, to preserve solvent integrity and enhance the overall sustainability of uranium extraction operations.

Keywords: Uranium, solvent extraction, alamine 336, degradation, oxidants, nitrosamines, ions.

Received: March 2025
Accepted: February 2026
Published: February 2026

1. Introduction

Uranium is a critical element for nuclear energy, and its extraction is an essential process for global energy production. At Rossing Uranium Limited (RUL), the recovery of uranium from acidic leach solutions relies on solvent extraction (SX), which selectively transfers uranium ions from the aqueous phase into the organic phase. The extractant Alamine 336 (N,N-dioctyl-1-octanamide) is widely used in the RUL SX circuit due to its efficiency, scalability, and stability (Kumar et al., 2011; Wehbie et al., 2021). However, under certain conditions, such as high acidity, elevated temperatures, and high ion concentrations, Alamine 336 can undergo degradation, leading to phase separation problems and the formation of unwanted by-products, such as crud (Chagnes and Cote, 2018; Forner et al., 2018; Vázquez-Campos et al., 2017). This degradation significantly impacts the efficiency of the extraction process and increases operational costs associated with solvent replacement and maintenance (Soldenhoff and Ring, 2007).

Solvent degradation at RUL is influenced by several factors, particularly the presence of various ions in the leach solution. While some ions, such as ferrous, are essential for redox control in the extraction process, others, like chloride, nitrate, and manganese, contribute to solvent degradation during later stages of the process. Ferrous ions maintain the ferric/ferrous ratio needed for redox control, while nitrates, originating from explosives used in mining, further exacerbate solvent degradation (Munyungano et al., 2008). Understanding the specific role of chloride, nitrate, ferrous, and manganese ions in this degradation process is essential to improving uranium extraction efficiency and reducing the costs associated with solvent degradation at RUL. Despite the importance of this issue, there is a lack of scientific reports on forced degradation studies of Alamine 336 in high ion concentration environments (Chagnes and Cote, 2018).

The degradation of Alamine 336 involves complex chemical reactions with various species in the leach solution, leading to the formation of by-products that alter the solvent's chemical composition. Radioactive species, such as uranium decay products, can also trigger chemical reactions that degrade the solvent (Guo et al., 2023). Additionally, high temperatures and pressures, which are typical in industrial operations, can accelerate these reactions, further contributing to solvent breakdown (Khanramaki et al., 2018; Zhu et al., 2016). Metal ions are key contributors to this degradation through several mechanisms, including complex formation, hydrolysis reactions, radical formation, and precipitation reactions. Metal ions can form complexes with Alamine 336, destabilizing it and leading to its breakdown (Sprakel and Schuur, 2023). Some ions catalyze hydrolysis reactions that produce acidic conditions, while others generate free radicals that react with Alamine 336, leading to its decomposition (Liu et al., 2014; Chagnes et al., 2011).

Nitrate ions have been identified as a significant contributor to Alamine 336 degradation by forming nitrosamines, which are toxic by-products that result from the reaction of nitrous acid with tertiary amines like Alamine 336 (Chen et al., 2018; Munyungano, 2007). Chloride ions also play a detrimental role by binding to the active sites of Alamine 336, reducing its ability to load uranium (Sole et al., 2011; Avelar et al., 2017). While chloride and nitrate ions have been widely studied for their impact on solvent degradation, the role of manganese in this process is less understood. Manganese is introduced into the SX circuit to help oxidize ferrous ions and facilitate uranium dissolution. However, manganese, particularly in the form of Mn^{2+}, may undergo redox reactions with the organic solvent, potentially accelerating Alamine 336 degradation (Van Lien et al., 2020). The concentration of manganese in RUL's raffinate and concentrated eluate is typically around 164–173 mg/L, and its impact on solvent stability warrants further investigation.

Despite the existing research on solvent degradation, many of the findings have yet to be fully implemented in the RUL SX process. A knowledge-based approach, such as factorial design, offers a promising solution for simultaneously examining the interactions between various ions while controlling experimental conditions. This approach can help identify the optimal parameters for minimizing Alamine 336 degradation, ultimately improving uranium extraction efficiency and reducing operational costs. By gaining a deeper understanding of the complex interactions between chloride, nitrate, ferrous, and manganese ions, this study aims to provide valuable insights that will help address the challenges of solvent degradation at RUL and optimize the overall extraction process.

2. Materials and Methods

2.1 Experimental Design

In this study, a 2^{k-p} fractional factorial design, like the one used by Chang et al., (2011); Gomes *et al*., (2015) and Sergis and Ouellet-Plamondon (2022), was employed to examine the impact of various ion concentration levels on the degradation of alamine 336. The selection of a fractional

factorial design for this research was motivated by the need to optimize limited resources while ensuring time and cost efficiency. Specifically, a quantitative 2^{k-p} factorial design was used, where k indicates the number of factors (4 in this case) and p reflects the degree of fractionation (2). This approach reduces the number of experiments from the full set of 16 to 8, facilitating the simultaneous investigation of the effects and interactions of various factors on alamine degradation.

The factors explored include low (2 g/L) and high (20 g/L) nitrate, low (1 g/L) and high (10 g/L) chloride, manganese at low (0.5 g/L) and high (5 g/L) concentrations, and ferrous ion at low (1 g/L) and high (5 g/L) levels. The experimental design aimed to quantify both the level and magnitude of interactions among these factors. The fractional factorial design table (Table 1) with the experimental plan provides the summary of the determination of the factors, the resolution, the number of runs, the number of replicates, the number of center points and the number of levels at which the experiments were carried out (Sergis and Ouellet-Plamondon, 2022).

Table 1. The fractional factorial design table with experimental plan

	Runs					
Factors	**4**	**8**	**16**	**32**	**64**	**128**
2	FULL					
3	III	FULL				
4		IV	FULL			
5		III	V	FULL		
6		III	IV	VI	FULL	
7		III	IV	IV	VII	FULL
8			IV	IV	VI	VIII
9			III	IV	IV	VI
10			III	IV	IV	VI
11			III	IV	IV	IV
12			III	IV	IV	V
13			III	IV	IV	V
14			III	IV	IV	IV
15			III	IV	IV	IV

The red labelled runs are the screening runs, while the green runs are full factorial designs, and the yellow are (IV) designs (fractional factorial). The three and four factor interactions are assumed to be zero. The selected IV design (circled), gives estimates of the average and the four main effects.

2.2 Analytical Techniques:

This section outlines the various techniques employed to assess the degradation of alamine 336, including titrimetric determinations, RDE-OES, ICP-OES, FTIR, and GC-MS analyses. A detailed examination of each method is provided.

2.2.1 Titrando Redox Potential Measurements

For redox potential measurements, the Metrohm 907 Titrando (P/N: 2.906.0010) with 815 Robotic sample processor XL (P/N: 2.815.0010) system was employed. Using Tiamo 2.5

software (like that by Allahdin *et al*., 2017). Once the analysis was completed, the report was displayed in the software and printed for record-keeping and data analysis.

2.2.2 Titrando Alamine Measurements

This analysis method utilizes the Metrohm 888 Titrando units with 801 stirrer and 803 titrations stand for amine determinations. A 20 ml aliquot of the sample from the degradation test was transferred into a 250 ml beaker. Methanol was added to bring the total volume to 150 ml. The Alamine analysis method as well as the alamine standard method was selected on the Titrino. The analysis was conducted by titrating the sample with 0.5 N perchloric acid. The titer volume (ml) was recorded, and a report was printed for alamine percentage calculation. After completing the titration, the electrode was rinsed with methanol.

Prior to determining alamine the factor was determined by using equation 1.

$$f = c/t \quad \text{(Eq. 1)}$$

where c = concentration (%) and t = titer in milliliters (ml).

Four alamine standards 5%, 7.5%, 9% and 10% alamine were analysed in triplicate and the average value for the factor for the individual standards was determined. The average factors for each of the standards were added together and divided by the number of factors used to obtain the average factor ($\bar{x}f$). The average factor is calculated as indicated in equation 2.

$$\bar{x}f = (f1+f2+f3+f4)/N \quad \text{(Eq. 2)}$$

Where:

$\bar{x}f$ = Average factor, $(f1+f2+f3+f4)$ = Sum of factors and N = number of standards used.

$$\text{Alamine (\%)} = \bar{x}f \text{ x titer (ml)} \quad \text{(Eq. 3)}$$

2.2.3 RDE-OES Analysis

Before analyzing samples, the RDE-OES was calibrated using a 0 ppm blank, a 100 ppm standard, and a 900 ppm standard, each measured five times to create a calibration line for Fe, Al, Cr, Cu, Tn, Pb, Ag, and Ni, Ca, Ba, Zn, P, Mg, B, Mb, Si, Na and K (van de Voort, 2022).

The RDE-OES employs an electric discharge method as the excitation source for the spectrometer (Miro *et al.,* 2017). The arc generated between two carbon electrodes ionizes the sample, emitting characteristic energies at specific wavelengths. A capacitor discharges across this gap, creating a high-temperature electric arc that vaporizes part of the sample, forming plasma. The emitted light contains emissions from all elements present in the sample. The intensity of the light measured is then converted into concentration values for the unknown sample. About 5ml sample was used for the analysis. The analysis took 30 to 40 seconds to be completed.

2.2.4 Oil Analysis with RDE Spectrometers

For analyzing organic solvents, a significant electric potential is established between two electrodes. Common electrode types include fixed tungsten or silver, as well as disk and rod graphite electrodes. The emissions produced are separated into individual wavelengths and measured using a specialized optical system. The rotating disk RDE technique is widely used for multi-elemental oil analysis, providing lab-quality results. RDE spectrometers can analyze up to 31 elements simultaneously in under a minute without solvents or gases. Their ease of use

and repeatability (3 to 6 percent RSD) make them ideal for condition monitoring in field workshops or less-than-ideal lab settings (Dhiman *et al*., 2019).

2.2.5 FTIR Handheld Infrared Analyzer

The FTIR handheld infrared oil analyzer is designed to assess the chemical and physical condition of oils, fuels, and lubricants. It measures components such as soot, Total Acid Number (TAN), Total Base Number (TBN), water, oxidation, sulfation, and nitration (van de Voort, 2022). With a library of around 850 different fluid spectra from around the globe, it has applications in various industries, including biodiesel and synthetic fuels.

This oxidation, sulphation and nitration values were obtained using the FluidScan 1100 Fourier Transform Infrared Spectrometer (P/N: FL367). Before sample analysis, a check fluid was analyzed to validate calibration and ensure the cleanliness of the lens. After successful calibration, a drop of the oil sample is placed on the reading window, and the appropriate program and oil type are selected. The analysis is then conducted, and takes about twenty seconds to complete. The analyzer can simultaneously assess up to 31 components and displays the results on-screen.

2.2.6 GC-MS Analysis of Forced Degradation Samples

Forced degradation samples were analyzed using a Shimadzu Gas Chromatography Mass Spectrometer system (P/N: GCMS-QP2020) in electron impact (EI) full scan mode, scanning a range of 50 to 600 m/z. Each sample was prepared by dissolving 10 µL in 1 mL of acetonitrile, followed by injecting 1 µL onto an SH-Rxi-5ms column (30 m, 0.25 mm ID, 0.25 µm). This method is similar to that used in prior studies at RUL (Munyungano *et al*., 2008). To ensure quality control, acetonitrile blanks were injected between samples to identify and eliminate any potential carryover. Autotuning and leak checks were performed before analysis. Data processing was conducted using LabSolutions software, with library searches performed using the NIST Library, and matched data presented in the subsequent section.

3. Results

3.1 Degradation Profiles of Alamine 336:

Nitrate and chloride as key predictors for the effect on alamine degradation.

The linear response surface reveals that nitrate and chloride are statistically significant predictors for alamine degradation, as shown in Figure 1. The values for manganese (Mn^{2+}) and ferrous ion (Fe^{2+}) were fixed at 2.75 g/L and 3 g/L, respectively. Notably, lower alamine concentrations are found in the lower right corner of the response surface, where nitrate levels are high, and chloride levels are moderate. This indicates that as nitrate concentrations rise, alamine degradation increases. Additionally, a higher concentration of chloride ions correlates with increased alamine concentration. These findings appear to contradict previous research, which indicated that chloride ions bind to the active sites of tertiary amines (Lunt *et al*., 2007), and concentrations exceeding 3 g/L are associated with detrimental effects on alamine loading (Forner *et al*., 2018).

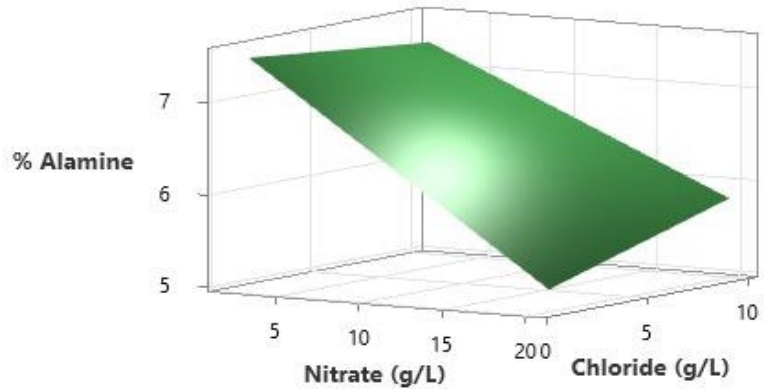

Figure 1. Surface plot for the effect of nitrates and chlorides on % alamine

Nitrate and Mn^{2+} predictors for the effect on alamine degradation

Figure 2 clearly shows that the lowest alamine concentration occurs in the lower right corner, where nitrate levels are high, and manganese levels are low. This reduction in alamine concentration may be linked to the oxidation of the organic solvent by nitrates (Hung *et al*., 2020). Additionally, the oxidizing effects of manganese dioxide (Munyungano *et al*., 2008; Van Lien *et al*., 2020) in conjunction with nitrates are known to adversely affect alamine in the solvent extraction circuit.

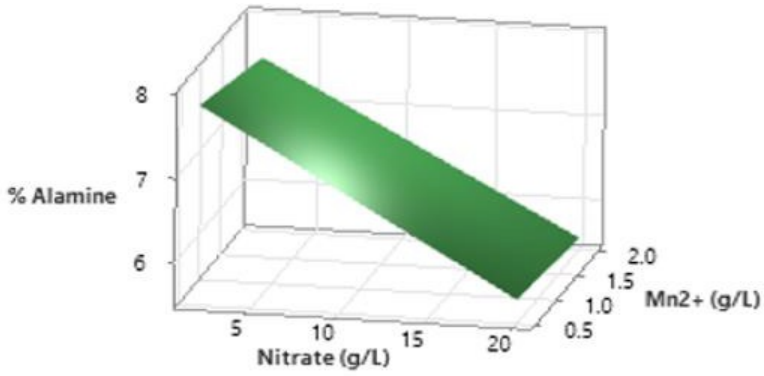

Figure 2. Surface plot for the effect of nitrates and manganese on % alamine

Nitrate and ferrous predictors for the effect on alamine degradation

Figure 3 indicates that the lowest alamine concentration is found in the lower left corner of the graph, where nitrate levels are high and ferrous levels are low. This suggests that an increase in nitrate concentration in the SX circuit corresponds to a decrease in alamine concentration due to oxidation of the amine. Nitrates have been associated with the oxidative degradation of alamine 336 (Munyungano, 2007; Soldenhoff and Ring, 2007; Chagnes and Courtaud, 2009b; Sole *et al*., 2011; Chagnes and Cote, 2018; Hung *et al*., 2020; Wehbie *et al*., 2021). Conversely, higher ferrous levels appear to support alamine stability, aligning with existing literature (Soldenhoff and Ring, 2007). These findings are upheld by prior studies suggesting that introducing ferrous

wire into the SX circuit enhances the ferrous-to-ferric ratio, thereby lowering the redox potential and reducing alamine degradation (Munyungano *et al*., 2008).

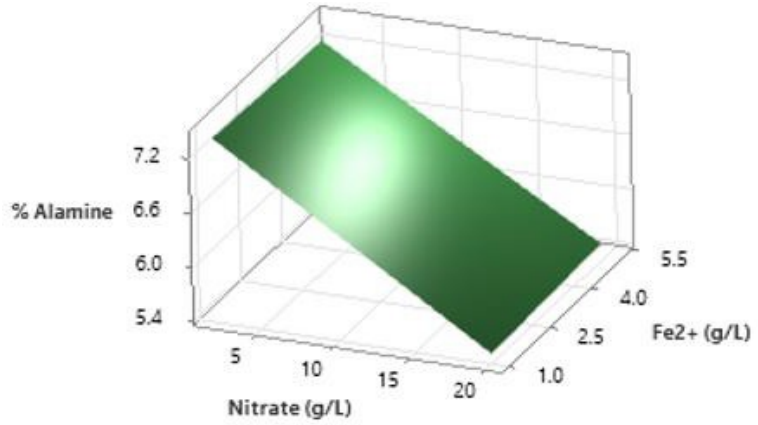

Figure 3. Surface plot for the effect of nitrates and ferrous on % alamine

Chloride and Mn^{2+} predictors for the effect on alamine degradation

From Figure 4, it may be deduced that the interaction between chloride and manganese ions has a moderate mutual effect on the chemical degradation of alamine. It can be inferred that the combined oxidising effects of chloride and manganese on alamine degradation is negligible.

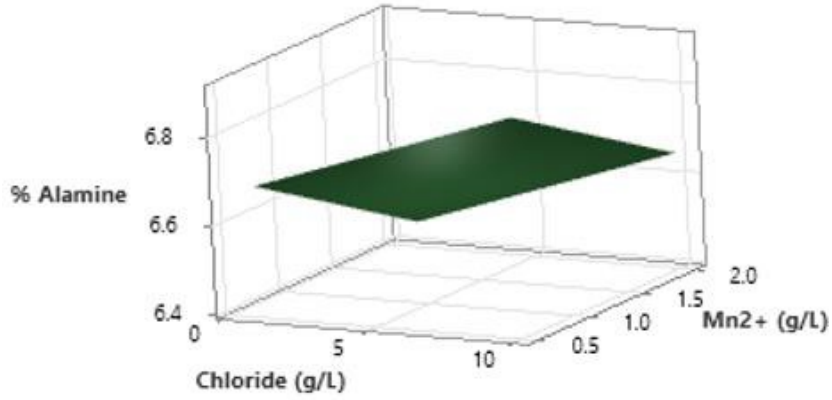

Figure 4. Surface plot for the effect of manganese and chlorides on % alamine

Effects of chloride and ferrous predictors for alamine degradation

In Figure 5, the lower values for alamine are at the bottom left corner which corresponds to low values for chloride and ferrous. This seems to indicate that higher values of chloride and ferrous in the concentrated eluate favour alamine health. Especially in the light of elevated hold values for nitrate (11 g/L) and the predictor values for chloride (10 g/L). The overall loss of alamine is almost negligible. This phenomenon supports the findings by Soldenhoff and Ring (2007).

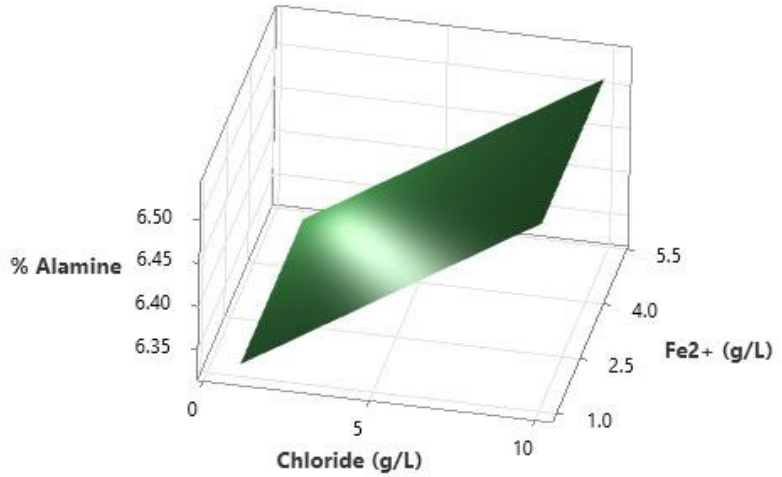

Figure 5. Surface plot for the effect of ferrous and chlorides on % alamine

The effects of manganese and ferrous as predictors for alamine degradation

Figure 6 illustrates the impact of manganese and ferrous on alamine degradation. The surface plots indicate that the lowest alamine concentration is found in the lower right corner, associated with high manganese levels and low ferrous levels. This suggests that increased manganese concentration reduces alamine levels, while low ferrous content in the concentrated eluate also contributes to this decrease. These observations are consistent with findings in the literature (Soldenhoff and Ring, 2007). However, despite the elevated levels of nitrate (11 g/L) and chloride (5.5 g/L), the overall loss of alamine remains minimal.

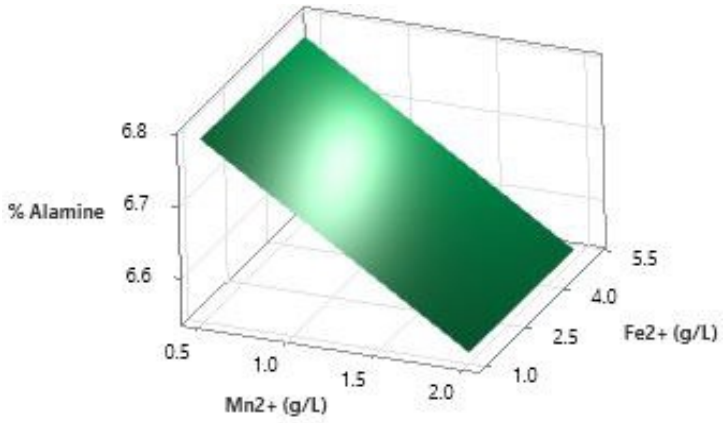

Figure 6. Surface plot for the effect of manganese and ferrous on % alamine

3.2 FTIR Spectroscopy analysis

The samples collected from the degradation process were analyzed using FTIR for oils. A 50 ml sample was filtered through Grade 1 Whatman filter paper to eliminate any particulate matter or contaminants. The sample was then homogenized. FTIR instrument introduces about 1ml sample directly via a peristaltic or syringe pump for analysis. The spectra are collected and processed, resulting in absorbance spectra for selected components. These systems are engineered to adhere to the ASTM FTIR protocols, setups, and operating procedures for

specific components according to designated wavelength regions and baselines outlined (van de Voort, 2022).

From the analysis, two samples (210055 and 21021), which did not undergo alamine losses, exhibited low levels of nitration, sulphation, and oxidation. Conversely, emulsions from the third phases extracted from samples 201025, 201025, and 201055 showed elevated values for nitration, sulphation, and oxidation. Additionally, the stripped solvent from the RUL processing plant, dated March 13, 2023, also displayed higher levels of oxidation, sulphation, and nitration.

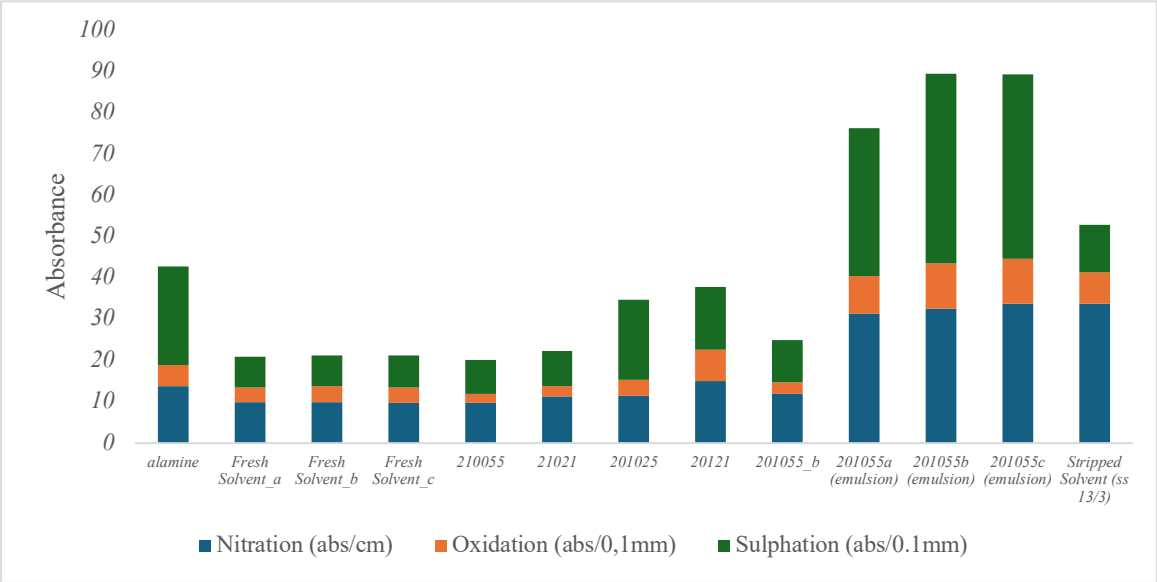

Figure 7. FTIR spectroscopic showing nitration, sulphation and oxidation data for selected samples.

3.3 GC-MS Data Summary

The GC-MS instrument detected several components in four out of the eight sample runs, as shown in Table 2 Among these were new components not previously found in the plant solvent containing pure alamine 336. These identified components includes a nitrosamine, N-Nitroso-di-n-octylamine, which supports findings from multiple authors (Soldenhoff and Ring, 2007; Munyungano *et al*., 2008; Chagnes and Cote, 2018; Chen *et al*., 2018). Additionally, N-Nitroso-di-n-octylamine, Hexanamide (N-ethyl-N-decyl), and 1-Octanamine-N-nitro-N-octyl were recognized as breakdown products of alamine 336. Aziridine, a component not present in the NIST Library database, was also identified in pure alamine 336 and is known to be used in the production of organic compounds (Chen *et al*., 2018).

Further, the results confirm that oxidation of alamine led to the formation of additional compounds namely Hexanamide (N-ethyl-N-decyl), Butyldidecylamine, and Cyclopentylmethylamine. The formation of nitrosamines observed aligns with findings from Munyungano *et al.* (2008), Chagnes and Cote (2018), and Chen *et al.* (2018).

Table 2: GC-MS data summary of the degradation samples obtained from the experiments.

Compound name	Ret. Time time	NIST % match	Formula	Chemical Class
1-Decanamine, N,N-didecyl	16.53	88	$C_{30}H_{63}N$	Amine
1-Octanamine, n-octyl	7.866	92	$C_{16}H_{35}N$	Amine

Alamine 336 (1-Octanamine, N,N-dioctyl)	13.764	75	$C_{24}H_{51}N$	Amine
Butyldioctylamine	9.271	77	$C_{20}H_{42}N$	Amine
Diheptylpentylamine	10.877	61	$C_{19}H_{41}N$	Amine
Formamide, N,N-dioctyl	8.121	66	$C_{17}H_{35}NO$	Amide
Isonipecotic acid, N-isobutoxycarbonyl-,undecyl ester	15.191	71	$C_{22}H_{41}NO_4$	Ester
Octanamide, N-heptyl-N-octyl	12.295	66	$C_{23}H_{47}NO$	Amide
Triisooctylamine	11.479	83	$C_{24}H_{51}N$	Amine
Tris(2-ethylhexyl)amine	12.241	89	$C_{24}H_{51}N$	Amine
1-Decanamine (N,N-didecyl)	16.528	85	$C_{30}H_{63}N$	Amine
1-Heptanamine, N,N-diheptyl	10.701	65	$C_{21}H_{45}N$	Amine
1-Octanamine (n-octyl)	7.867	95	$C_{16}H_{35}N$	Amine
1-Octanamine, (N-nitro-N-octyl)	12.236	73	$C_{16}H_{34}N_2O_2$	Nitroamine
2-Cyclohexyl-N1,N1,N4,N4-tetraisobutyl- 3-methyl-succinamide	14.261	62	$C_{27}H_{52}N_2O_2$	Amide
2-Methyldocosane	12.15	74	$C_{23}H_{48}$	Alkane
4-Methoxy-6(1-pyrolidinylmethyl), (1,1,5-Triazin-2-amine)	7.511	77	$C_9H_{15}N_5O$	Amine
Aziridine, 2-(1,1-dimethylethyl)-1-hexyl-3-methyl-, trans)	9.005	75	$C_{13}H_{27}N$	-
Butyldidecylamine	12.458	73	$C_{24}H_{51}N$	Amine
Butyldioctylamine	9.27	81	$C_{20}H_{43}N$	Amine
Cyclopentylmethylamine, N,N-dinonyl	13.034	72	$C_{24}H_{49}N$	Amine
Dibutyl phthalate	9.575	93	$C_{16}H_{22}O_4$	Phthalate
Diheptylpentylamine	10.875	67	$C_{19}H_{41}N$	Amine
Diisooctyl phthalate	14.325	84	$C_{24}H_{38}O_4$	Phthalate
di-n-Decylamine	11.09	78	$C_{20}H_{43}N$	Amine
Ethylamine, N,N diheptyl-2-(2-thiophenyl)	10.705	66	$C_{20}H_{37}NS$	Amine
Hexanamide, N-ethyl-N-decyl	11.571	64	$C_{18}H_{37}NO$	Amide
Isonipecotic acid (N-isobutoxycarbonyl undecyl ester)	15.188	71	$C_{22}H_{41}NO_4$	Ester
N-Ethyl-4-propyl-4-nonanamine	9.425	78	$C_{14}H_{31}N$	Amine
N-Ethyl-6-propyl-6-tridecanamine	9.67	71	$C_{18}H_{39}N$	Amine
N-Nitroso-di-n-octylamine	10.452	90	$C_{16}H_{34}N_2O$	Nitrosamine
Octahydrochrom-4,5-dione, 4',8'-epoxy	15.651	63	$C_{18}H_{28}O_4$	-
Octanamide, N-heptyl-N-octyl	12.29	67	$C_{23}H_{47}NO$	Amide
Phenanthrene	7.658	88	$C_{14}H_{10}$	PAH
Propyl N- (heptafluorobutyryl) pyroglutamate	12.764	71	$C_{12}H_{12}F_7NO_4$	-
Pyrene	11.115	74	$C_{16}H_{10}$	PAH
Tris(2-ethylhexylamine)	12.442	90	$C_{24}H_{51}N$	Amine
Isonipecotic acid, N-isobutoxycarbonyl-,heptylester	10.701	76	$C_{18}H_{33}NO_4$	Ester

Octahydrochrom-4,5-dione, 4',8'-epoxy-	15.651	63	$C_{18}H_{28}O_4$	-
Triisooctylamine	11.478	88	$C_{24}H_{51}N$	Amine

3.4 Factorial regression for the test statistic for alamine

The factorial regression for the test statistic for alamine is shown in the Table 3.

Table 3. ANOVA table for the factorial regression for the test statistic for alamine

Source	DF	Adj SS	Adj MS	F-Value	P-Value
Model	7	26.0333	3.71905	549.61	0.000
Linear	4	4.6933	1.17332	173.40	0.000
Nitrate (g/L)	1	4.0996	4.09960	605.85	0.000
Chloride (g/L)	1	0.2481	0.24807	36.66	0.000
Mn^{2+} (g/L)	1	0.3456	0.34560	51.07	0.000
Fe^{2+} (g/L)	1	0.0000	0.00002	0.00	0.961
2-Way Interactions	3	1.0783	0.35943	53.12	0.000
Nitrate (g/L)*Chloride (g/L)	1	1.0086	1.00860	149.05	0.000
Nitrate (g/L)*Mn^{2+} (g/L)	1	0.0417	0.04167	6.16	0.025
Nitrate (g/L)*Fe^{2+} (g/L)	1	0.0280	0.02802	4.14	0.059
Error	16	0.1083	0.00677		
Total	23	26.1416			

From Table 3 we can infer that the model is orthogonal such that the effect of some factors balances out across the effects of the other factors. Regression equation in uncoded units for alamine 336 is given by equation 4.

% Alamine=8.4313 – 0.15319 Nitrate (g/L) – 0.03309 Chloride (g/L) – 0.2279 Mn^{2+} (g/L) – 0.0213 Fe^{2+} (g/L) + 0.005062 Nitrate (g/L)*Chloride (g/L) + 0.00617 Nitrate (g/L)*Mn^{2+} (g/L) + 0.001898 Nitrate (g/L)*Fe^{2+} (g/L)

(Eq. 4)

3.5 Interaction Effects:

The analysis of the interaction effects was conducted to determine how the simultaneous presence of multiple ions affects the degradation of alamine 336. Standardized effect charts as shown in Figure 8 illustrate the influence of the four factors and their interactions on alamine 336 which is the response variable. The interaction plot in Figure 8 was created using the backward selection method in Minitab, applying a significance level of $\alpha = 0.10$ for variable removal. The standardized effects reflect the changes in alamine concentration due to individual factors while keeping others constant. These effects are determined by dividing the measured effect by the standard deviation of alamine concentration.

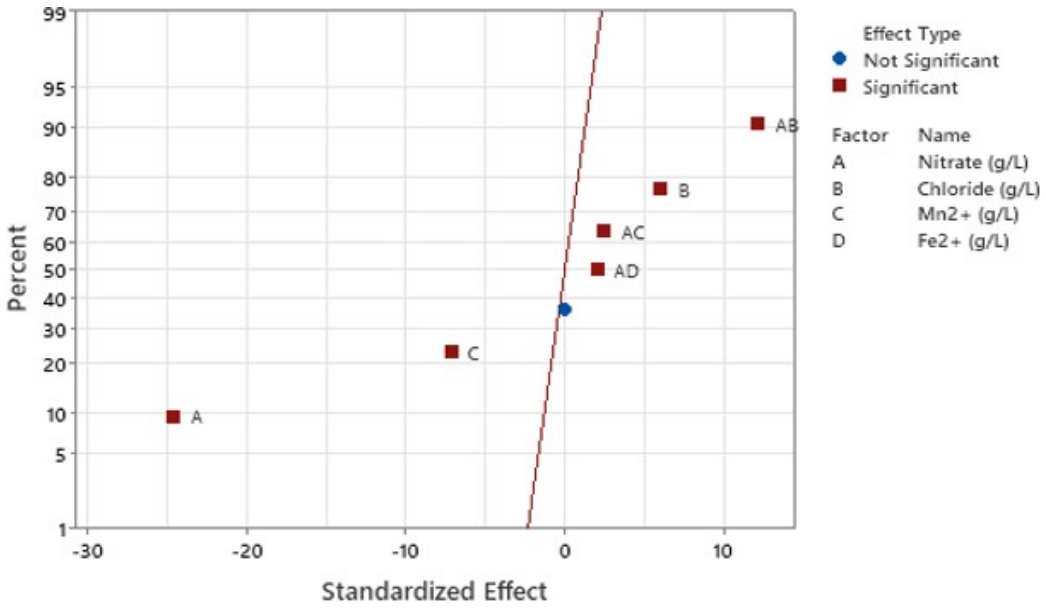

Figure 8. Normal plot for the standardized effects for alamine (α =0.10)

The main effects of nitrate, chloride, and manganese on alamine concentration are statistically significant at the α = 0.10 level. Notably, chloride has the highest positive contribution (76%) to the variation in alamine concentration, indicating that increasing chloride levels raises alamine concentration. This finding appears to contradict previous research by Avelar et al. (2017), which suggested that higher chloride concentrations reduce alamine 336's uranium extraction efficiency.

Conversely, both nitrate and manganese show negative standardized effects, meaning that as their concentrations increase, the alamine concentration decreases. The impact of ferrous ions on alamine degradation is insignificant, aligning with earlier studies by Soldenhoff and Ring (2007). This is expected since nitrate (-0.282 mV/K) and manganese (-1.61 mV/K) have more negative electrode potentials, allowing them to more readily release electrons and act as oxidizing agents.

The interaction effects between nitrate and manganese, nitrate and chloride, and nitrate and ferrous show a positive correlation with alamine concentration; as their levels rise, so does alamine concentration. Thus, manganese (22%) has the most significant effect on alamine degradation, while nitrate (10%) also contributes significantly. While previous studies have supported the role of nitrates in alamine degradation (Munyungano *et al*., 2008; Sole *et al*., 2011), this study highlights that manganese in concentrated eluate is a major contributor to alamine degradation. This finding is particularly significant given the limited literature on manganese's role in solvent degradation. It is possible that manganese acts as a catalyst in certain reactions, facilitates solvent loss, participates in redox reactions (Van Lien *et al*., 2020), or forms complexes with alamine 336, potentially leading to solvent breakdown.

3.6 Multiple response predictors for alamine degradation at 95% confidence interval

The desirability function model predicts operating conditions *x* for the output variable, d that provide the "most desirable" response values. If d= 0 the conditions are completely undesirable and when d = 1 the conditions are the most desirable. The vertical bars can be moved to change

the factor settings and thereby change the individual desirability (d) of the responses and the composite desirability. From the model shown in Figure 9, nitrates have the most significant effect on alamine desirability while ferrous (Fe^{2+}) has little or limited effect on alamine degradation.

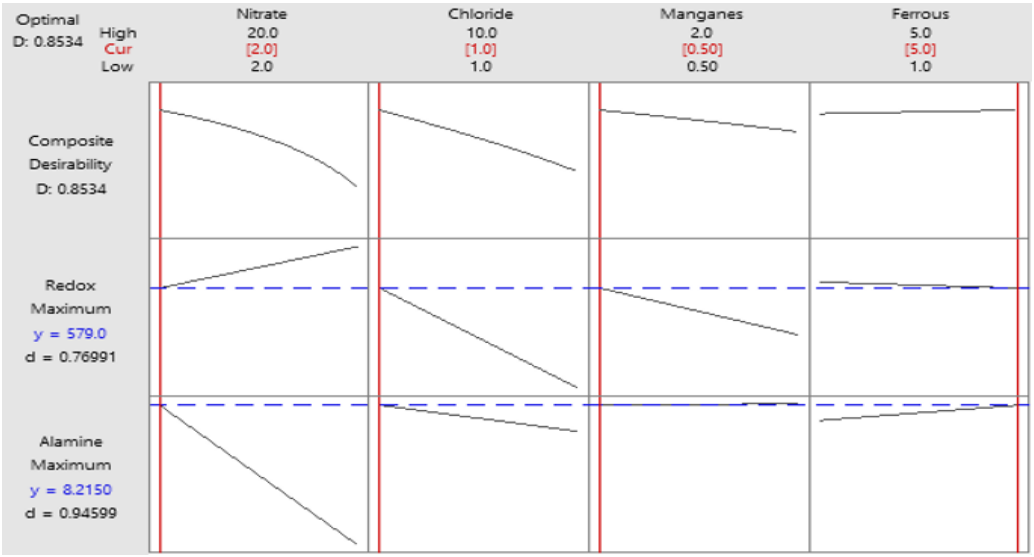

Figure 9. Multiple response predictors for alamine at 95% confidence interval

4. Discussion

The results of this study provide valuable insights into the degradation profiles of Alamine 336 in the solvent extraction process at Rossing Uranium Limited (RUL), highlighting the significant influence of various ions, such as nitrate, chloride, manganese, and ferrous ions, on the solvent's stability. Several factors and their interactions were identified as critical determinants of Alamine degradation, with nitrate and chloride ions emerging as key predictors.

Nitrate and chloride ions have been found to significantly affect Alamine 336 degradation. The linear response surface (Figure 1) illustrates that increasing nitrate concentrations correlate with higher levels of Alamine degradation. Notably, when nitrate levels rise, a decrease in Alamine concentration occurs, aligning with previous studies that have associated nitrates with the oxidative degradation of Alamine 336 (Munyungano, 2007; Soldenhoff and Ring, 2007; Chagnes and Cote, 2018). This is consistent with the idea that nitrate, acting as an oxidizing agent, can destabilize the organic solvent. Interestingly, the data also suggest that higher chloride concentrations correlate with increased Alamine concentrations, which seems to contradict prior research indicating that chloride ions bind to the active sites of tertiary amines (Lunt et al., 2007). However, these findings can be understood in the context of the complex interactions between ions, as chloride's role in the extraction process may be more nuanced than previously suggested. Further research is needed to resolve these conflicting results, particularly regarding the role of chloride in Alamine degradation.

The combination of nitrate and manganese also significantly affects Alamine 336 degradation. Figure 2 shows that low Alamine concentrations are observed in the lower right corner of the response surface, where nitrate levels are high, and manganese levels are low. This reduction in Alamine concentration may be due to the combined oxidative effects of nitrates and manganese (Munyungano et al., 2008; Van Lien et al., 2020). Manganese, particularly in the form of

manganese dioxide, has been shown to catalyze oxidation reactions that degrade Alamine 336, and the synergistic effect of nitrate and manganese is likely a key contributor to the observed degradation.

Ferrous ions, which play an essential role in maintaining the ferric/ferrous ratio for redox control, were found to have a stabilizing effect on Alamine 336. Figure 3 shows that higher ferrous concentrations are associated with higher Alamine concentrations, indicating that the presence of ferrous ions helps to maintain solvent integrity by reducing the redox potential. This finding supports the existing literature, which suggests that maintaining a balanced ferrous-to-ferric ratio in the SX circuit can mitigate Alamine degradation (Soldenhoff and Ring, 2007; Munyungano et al., 2008). The results reinforce the importance of managing ferrous ion levels to enhance the stability of Alamine 336 and reduce the costs associated with solvent degradation.

The interaction between chloride and manganese ions has a moderate effect on Alamine degradation, as indicated in Figure 4. This interaction appears to have a relatively negligible impact on the degradation of Alamine 336, suggesting that while both ions can contribute to solvent breakdown, their combined effect is less significant compared to nitrate or ferrous ions. This finding contrasts with other studies that have highlighted the combined oxidizing effects of chloride and manganese (Soldenhoff and Ring, 2007), but the data here indicate that the impact of this interaction is more complex and warrants further investigation.

The combined effect of chloride and ferrous ions (Figure 5) shows that higher concentrations of both ions tend to stabilize Alamine 336, leading to minimal degradation. The presence of high chloride and ferrous concentrations in the concentrated eluate appears to favor solvent stability, with the overall loss of Alamine being almost negligible. This result supports previous findings by Soldenhoff and Ring (2007), who observed that chloride and ferrous ions in the correct proportions can help maintain solvent integrity in the SX circuit.

Finally, the interaction between manganese and ferrous ions (Figure 6) highlights that increased manganese concentrations lead to a reduction in Alamine concentration, while low ferrous levels exacerbate this effect. These findings are consistent with earlier studies (Soldenhoff and Ring, 2007) and suggest that manganese acts as a key contributor to Alamine degradation in the SX circuit. Despite elevated levels of nitrate and chloride, which typically contribute to degradation, the overall loss of Alamine remains minimal when manganese and ferrous ions are managed appropriately.

The FTIR and GC-MS analysis further corroborate the observed degradation trends. FTIR analysis of the degradation process revealed that samples without significant Alamine losses showed low levels of nitration, sulphation, and oxidation, while emulsions from samples with significant degradation exhibited elevated levels of these chemical reactions (Figure 7). This supports the hypothesis that nitration, sulphation, and oxidation are key chemical processes involved in Alamine degradation. The GC-MS data identified several new degradation products, including N-Nitroso-di-n-octylamine, which has been previously reported as a breakdown product of Alamine 336 (Soldenhoff and Ring, 2007; Munyungano et al., 2008; Chagnes and Cote, 2018). The identification of these degradation products further validates the findings from the surface plots and suggests that oxidative processes, catalyzed by ions such as nitrate and manganese, play a significant role in Alamine breakdown.

Factorial regression analysis (Table 3) provided a clear statistical model for predicting Alamine degradation based on ion concentrations. The results indicated that nitrate, chloride, and

manganese had significant effects on Alamine degradation, with nitrate having the most substantial influence. The regression equation derived from the analysis (Equation 4) offers a predictive tool for optimizing solvent extraction conditions, highlighting the importance of controlling ion concentrations to minimize Alamine degradation. Additionally, the interaction effects between nitrate and manganese, nitrate and chloride, and nitrate and ferrous ions were found to contribute significantly to Alamine degradation, emphasizing the complexity of the degradation process and the need for precise control of multiple factors in the SX circuit.

In conclusion, this study demonstrates that nitrate, chloride, manganese, and ferrous ions play critical roles in the degradation of Alamine 336 during the uranium extraction process at RUL. Nitrate and manganese, in particular, emerge as key contributors to oxidative degradation, while ferrous ions help stabilize the solvent. The factorial regression model provides a useful tool for predicting Alamine degradation based on ion concentrations, and the findings highlight the importance of managing these ions in the SX circuit to enhance solvent stability and improve extraction efficiency.

5. Conclusion

In conclusion, this study has highlighted the significant role of oxidants, such as nitrates, chlorides, and manganese ions, in the degradation of Alamine 336 during the solvent extraction process at Rossing Uranium Limited (RUL). Nitrates were identified as the primary driver of Alamine breakdown through acidic hydrolysis and oxidation, with manganese acting as a secondary oxidant, mitigating the impact of ferrous ions while also contributing to solvent degradation. Chlorides, while thought to inhibit solvent efficiency in previous studies, were found to have a more complex role in the RUL system, with their presence correlating with higher Alamine concentrations in some cases. The formation of emulsions and the occurrence of solvent degradation in samples with high redox potentials further reinforced the connection between high redox values and the breakdown of the organic solvent. Overall, the findings suggest that careful management of ion concentrations, particularly nitrates and manganese, is essential to maintaining the stability of Alamine 336 and enhancing uranium extraction efficiency.

For future research, pilot plant trials should be conducted to evaluate the feasibility of using chlorides to control solvent degradation and assess the economic implications of chloride use, balancing potential cost savings from reduced degradation with any additional costs. Additionally, methods to reduce nitrate, ferrous, and manganese concentrations in the processing circuit should be explored, including the implementation of membrane filtration systems for effective nitrate removal. A quantitative monitoring system, such as GC-MS, should be established to closely track the formation of solvent degradation products like nitrosamines and nitroamines. This would allow for real-time detection and management of degradation issues, contributing to more efficient solvent management and improved overall performance of the solvent extraction process at RUL.

REFERENCES

Allahdin, O., Mabingui, J., Wartel, M., Boughriet, A., 2017. Removal of Pb^{2+} ions from aqueous solutions by fixed-BED column using a modified brick: (Micro) structural, electrokinetic and mechanistic aspects. Applied Clay Science 148, 56-67.

Avelar, E.C., Alvarenga, C.L.G., Resende, G.P.S., Morais, C.A., Mansur, M.B., 2017. Modeling of the solvent extraction equilibrium of uranium (VI) sulfate with Alamine 336. Brazilian Journal of Chemical Engineering 34, 355-362.

Chagnes, A., Cote, G., 2018. Chemical Degradation of a Mixture of tri-n-Octylamine and 1-Tridecanol in the Presence of Chromium (VI) in Acidic Sulfate Media. Metals 8, 57.

Chagnes, A., Fosse, C., Courtaud, B., Thiry, J., Cote, G., 2011. Chemical degradation of trioctylamine and 1-tridecanol phase modifier in acidic sulfate media in the presence of vanadium (V). Hydrometallurgy 105, 328-333.

Chang, S.H., Teng, T.T., Norli, I., 2011. Screening of factors influencing Cu (II) extraction by soybean oil-based organic solvents using fractional factorial design. Journal of Environmental Management 92, 2580-2585.

Chen, X., Huang, G., An, C., Yao, Y. and Zhao, S., 2018. Emerging N-nitrosamines and N-nitramines from amine-based post-combustion CO_2 capture–a review. Chemical Engineering Journal 335, 921-935.

Dhiman, C., Paliwal, A., Khan, M.S., Reddy, M.N., Gupta, V., Tomar, M., 2019. Detailed Sensitive Detection of Impurities in Waste Engine Oils Using Laser Induced Breakdown Spectroscopy, Rotating Disk Electrode Optical Emission Spectroscopy and Surface Plasmon Resonance. International Journal of Physical and Mathematical Sciences 13, 167-172.

Forner, E.L., Archer, S.J., Coetzee, V.E., Soldenhoff, K., Quinn, J., 2018. Uranium recovery from high-chloride sulphate leach solutions: A cost tradeoff study of using treated water vs. saline water as make-up water. Journal of the Southern African Institute of Mining and Metallurgy 118, 95-102.

Gomes, Y.F., Medeiros, P.N., Bomio, M.R.D., Santos, I.M.G.D., Paskocimas, C.A., Nascimento, R.M.D., Motta, F.V.D., 2015. Optimizing the synthesis of cobalt aluminate pigment using fractional factorial design. Ceramics International 41, 699-706.

Guo, Q., Chen, Y., Zhang, P., Liu, Y., Li, Y., Yang, Y., Cao, Q., Lin, M., 2023. The effects of structural variations in neutral phosphorus extractants on UO_2^{2+} extraction behavior and radiation stability: experimental and theoretical insights. Journal of Molecular Liquids 388, 122785.

Hung, N.T., Thuan, L.B., Thanh, T.C., Watanabe, M., Van Khoai, D., Thuy, N.T., Nhuan, H., Minh, P.Q., Mai, T.H., Van Tung, N., Tra, D.T.T., 2020. Separation of thorium and uranium from xenotime leach solutions by solvent extraction using primary and tertiary amines. Hydrometallurgy 198, 105506.

Khanramaki, F., Shirani, A.S., Safdari, J., Torkaman, R., 2017. Equilibrium and kinetics of uranium (VI) extraction from a sulfate leach liquor solution by Alamine 336 using single drop technique. Chemical Engineering Research and Design 125, 181-189.

Kumar, J.R., Kim, J.S., Lee, J.Y., Yoon, H.S., 2011. A brief review on solvent extraction of uranium from acidic solutions. Separation & Purification Reviews 40, 77-125.

Liu, Y., Zhao, D., Zhao, Z.Z., 2014. Study of degradation mechanisms of cyclobenzaprine by LC-MS/MS. Analytical Methods 6, 2320-2330.

Lunt, D., Boshoff, P., Boylett, M., El-Ansary, Z., 2007. Uranium extraction: the key process drivers. Journal of the Southern African Institute of Mining and Metallurgy 107, 419-426.

Miró Mezquita, G., Tormos, B., Allmaier, H., Knauder, C., 2017. Current trends in ICE wear detection technologies: From lab to field. ASRO Journal of Applied Mechanics 2, 32-41.

Munyungano, B., Feather, A., Virnig, M., 2008. *Degradation problems with the solvent extraction organic at Rössing uranium*. International Conference on Solvent Extraction. United States of America.

Munyungano, B.M., 2007. Solvent degradation-rossing uranium mine. Journal of the Southern African Institute of Mining and Metallurgy 107, 415-417.

Sergis, V., Ouellet-Plamondon, C.M., 2022. Fractional factorial design to study admixtures used for 3D concrete printing applications. Materials Letters 324, 132697.

Soldenhoff, K., Ring, R., 2007. *A Report to Rio Tinto on Recommendations arising from the ANSTO site visit to Rossing Uranium Mines*. Sydney. Available at: https://www.ansto.gov.au/sites/default/files/2019-12/Minerals%20Uranium%20Processing%20Capability%20Statement%20Dec19.pdf. Accessed date: 20 December 2024.

Sole, K.C., Cole, P.M., Feather, A.M., Kotze, M.H., 2011. Solvent extraction and ion exchange applications in Africa's resurging uranium industry: a review. Solvent extraction and ion exchange 29, 868-899.

Sprakel, L.M.J., Schuur, B., 2019. Solvent developments for liquid-liquid extraction of carboxylic acids in perspective. Separation and purification technology, 211, 935-957.

Van de Voort, F.R., 2022. FTIR Condition Monitoring of In-Service Lubricants: Analytical Role and Quantitative Evolution. Tribology Online 17, 144-161.

Van Lien, T., Dinh, T.T., Dung, N.T.K., 2020. Study on leaching systems and recovery for PALUA–PARONG low grade uranium sandstone ores. Hydrometallurgy 191, 105164.

Vázquez-Campos, X., Kinsela, A.S., Collins, R.N., Neilan, B.A., Waite, T.D., 2017. Uranium extraction from a low-grade, stockpiled, non-sulfidic ore: Impact of added iron and the native microbial consortia. Hydrometallurgy 167, 81-91.

Wehbie, M., Arrachart, G., Sukhbaatar, T., Le Goff, X.F., Karamé, I. and Pellet-Rostaing, S., 2021. Extraction of uranium from sulfuric acid media using amino-diamide extractants. Hydrometallurgy 200, 105550.